TISSUE ENGINEERING: Part C
Volume 22, Number 8, 2016

DOI: 10.1089/ten.tec.2016.0109

termis
Tissue Engineering
& Regenerative Medicine
International Society

METHODS ARTICLE

Comparative Decellularization and Recellularization of Wild-Type and Alpha 1,3 Galactosyltransferase Knockout Pig Lungs: A Model for *Ex Vivo* Xenogeneic Lung Bioengineering and Transplantation

Joseph Platz, MD,[1,*] Nicholas R. Bonenfant, BS,[1,*] Franziska E. Uhl, PhD,[1] Amy L. Coffey, MS,[1] Tristan McKnight, BA,[1] Charles Parsons, MD,[1] Dino Sokocevic, BA,[1] Zachary D. Borg, BA,[1] Ying-Wai Lam, PhD,[2] Bin Deng, PhD,[2] Julia G. Fields, BA,[2] Michael DeSarno, PhD,[3] Roberto Loi, PhD,[4] Andrew M. Hoffman, DVM, DVSc, DACVIM,[5] John Bianchi, PhD,[6] Brian Dacken, BA,[7] Thomas Petersen, MD, PhD,[8] Darcy E. Wagner, PhD,[1,9] and Daniel J. Weiss, MD, PhD[1]

Background: A novel potential approach for lung transplantation could be to utilize xenogeneic decellularized pig lung scaffolds that are recellularized with human lung cells. However, pig tissues express several immunogenic proteins, notably galactosylated cell surface glycoproteins resulting from alpha 1,3 galactosyltransferase (α-gal) activity, that could conceivably prevent effective use. Use of lungs from α-gal knock out (α-gal KO) pigs presents a potential alternative and thus comparative de- and recellularization of wild-type and α-gal KO pig lungs was assessed.
Methods: Decellularized lungs were compared by histologic, immunohistochemical, and mass spectrometric techniques. Recellularization was assessed following compartmental inoculation of human lung bronchial epithelial cells, human lung fibroblasts, human bone marrow-derived mesenchymal stromal cells (all via airway inoculation), and human pulmonary vascular endothelial cells (CBF) (vascular inoculation).
Results: No obvious differences in histologic structure was observed but an approximate 25% difference in retention of residual proteins was determined between decellularized wild-type and α-gal KO pig lungs, including retention of α-galactosylated epitopes in acellular wild-type pig lungs. However, robust initial recellularization and subsequent growth and proliferation was observed for all cell types with no obvious differences between cells seeded into wild-type versus α-gal KO lungs.
Conclusion: These proof of concept studies demonstrate that decellularized wild-type and α-gal KO pig lungs can be comparably decellularized and comparably support initial growth of human lung cells, despite some differences in retained proteins. α-Gal KO pig lungs are a suitable platform for further studies of xenogeneic lung regeneration.

[1]Department of Medicine, University of Vermont College of Medicine, Burlington, Vermont.
[2]Department of Biology and VGN Proteomics Facility, University of Vermont College of Arts and Sciences, Burlington, Vermont.
[3]Biostatistics Unit, University of Vermont College of Medicine, Burlington, Vermont.
[4]Department of Biomedical Sciences, University of Cagliari, Cagliari, Italy.
[5]Department of Clinical Sciences, Tufts University, Cummings School of Veterinary Medicine, North Grafton, Massachusetts.
[6]Revivicor, Inc., Blacksburg, Virginia.
[7]Exemplar Genetics, Sioux Center, Iowa.
[8]United Therapeutics Corp., Research Triangle Park, Durham, North Carolina.
[9]Comprehensive Pneumonology Center, Helmholtz Center Munich, Ludwig Maximilians University Munich, Munich, Germany.
*These authors are co-first authors.

Introduction

Approximately 1000–1500 lung transplants per year are performed in the United States, but a significant shortage of suitable donor lungs and the drawbacks of lung transplantation, including lifelong immunosuppression and an approximate 50% 5-year mortality, demonstrates the critical need for new approaches.[1] Use of acellular lung scaffolds for *ex vivo* lung bioengineering has been increasingly investigated as an alternative approach that could potentially allow use of cadaveric or otherwise suboptimal donor lungs following decellularization and seeding with autologous stem or progenitor cells obtained from the eventual transplant recipients (reviewed in Prakash *et al.*,[2] Calle *et al.*,[3] and Wagner *et al.*[4]). In particular, recent progress with decellularization and initial recellularization of human lungs has demonstrated the potential feasibility of this approach.[5–11] However, not all cadaveric or suboptimal donor lungs may be suitable. In particular, those that originate from aged donors, donors with preexisting structural lung diseases, or a combination of both age and lung disease may not be suitable. For example, we have recently found that emphysematous changes impair recellularization of both rodent and human lungs and that aging and emphysematous injury further impaired recellularization in rodent models.[10,12] Other work has demonstrated that decellularized human lung scaffolds obtained from patients with idiopathic pulmonary fibrosis (IPF) promote a fibrotic phenotype (myofibroblast differentiation) of inoculated fibroblasts.[6,13] Therefore, it is unlikely that lungs with any sort of preexisting lung disease could be used in a clinical translation scheme. This significantly limits the supply of lungs to be conceivably used in de- and recellularization approaches.

One potential alternative is to utilize a xenogeneic approach for lung decellularization and recellularization. Ideally, the lungs would be procured from a readily available animal source, which shares structural and physiologic attributes of human lungs, for which there are no potential ethical or other concerns, and that have minimal antigenic mismatch. To this end, domestic pigs (*Sus scrofa*) may provide a viable option as the size and general anatomy of adult pig lungs are conducive to consideration for use in human transplantation. Use of acellular pig lung scaffolds is thus an appealing option but brings additional challenges with respect to xenogeneic antigens. The alpha (1,3)-galactose (α-gal) epitope on glycolipids and glycoproteins is the major porcine xenoantigen recognized by xenoantibodies.[14,15] This epitope is formed by alpha (1,3)-galactosyltransferase, which is present in all mammals except man, apes, and Old World monkeys.[14,15] Both preclinical and clinical data demonstrate that following processing of other porcine tissues, such as heart valves and dermal grafts, both native and decellularized tissues may contain residual α-galactosylated proteins that contribute to immune response and graft failures.[16–20] One significant concern therefore is that acellular pig lung scaffolds might also contain residual immunogenic galactosylated proteins. One strategy utilized has been to treat native or acellular grafts with α-galactosidase to remove any residual α-galactosylated epitopes.[21,22] Another strategy has been to utilize tissues arising from transgenic pigs that lack expression of this enzyme (α-gal knock out [α-gal KO]); heart valves and dermal grafts obtained from α-gal KO pigs are significantly less immunogenic.[23] As such, use of acellular lungs from α-gal KO pigs offers a potentially less immunogenic scaffold for xenogeneic consideration.

We therefore conducted an initial investigation as to whether decellularized α-gal KO pig lungs recellularized with human cells might present a viable option for consideration in developing strategies for use in clinical bioartificial lung transplantation. Using an optimized detergent-based protocol developed for large (human and pig) lungs, decellularized wild-type versus α-gal KO pig lungs were comparatively assessed using histologic, immunohistochemical (IHC), and mass spectrometric analyses.[9–11] We then utilized a high-throughput approach for seeding alginate-coated decellularized lung segments through physiologically relevant seeding routes[11] and assessed initial growth and subsequent behavior over a 4-week period between wild-type and α-gal KO pig lungs using four different relevant human cell types: human bronchial epithelial (HBE) cells, human lung fibroblasts (HLF), human bone marrow-derived mesenchymal stromal cells (hMSCs), and human pulmonary vascular endothelial cells (CBF).

Results

Decellularized wild-type and α-gal KO pig lungs have similar gross histologic appearance and qualitatively retain most major extracellular matrix proteins by histologic and IHC evaluations

Using an optimized Triton X-100/sodium deoxycholate (SDC) detergent-based decellularization protocol with constant flow perfusion (2 L/min) of both the vasculature and airways, wild-type and α-gal KO pig lungs underwent parallel successful decellularization as gauged by progressive loss of pink coloration and a final translucent pearly white appearance (Fig. 1). The details of the decellularization protocol including rinse volumes are presented in Supplementary Table S1 (Supplementary Data are available online at www.liebertpub.com/tec).

One important endpoint in whole lung decellularization is the maintenance of major airway and vascular structures and basement membrane composition, while removing cells and clearing cellular material. Following decellularization of both wild-type and α-gal KO pig lungs, we observed similar maintenance of the major histologic and extracellular matrix (ECM) structures as assessed by hematoxylin and eosin (H&E), Verhoeff's Van Gieson (EVG), Masson's trichrome, and Alcian blue stains (Fig. 2A). As previously noted in decellularized rodent, nonhuman primate, and human lungs, there is qualitative loss of elastin as assessed by the EVG stain.[9–12,24–26] Similarly, we observed a qualitative loss of lung glycosaminoglycans, many of which are likely cell-associated, as assessed by Alcian blue staining (Fig. 2A). Transmission electron microscopy demonstrated no obvious difference in ultrastructural architecture between decellularized wild-type and α-gal KO pig lungs and confirmed maintenance of the alveolar structure, despite the use of pumps and higher flow rates (Fig. 2B). Minimal residual DNA was observed in decellularized wild-type and α-gal KO pig lungs as assessed qualitatively on DNA gels (Fig. 2C).

We further evaluated detergent concentration in the effluents during decellularization from four wild-type and two α-gal KO pig lung decellularizations. The wild-type data were previously published but displayed at absolute absorbance.[27] SDC concentration was reduced in the effluents with each consecutive wash step after incubation in SDC overnight. We found no significant difference in detergent concentrations between the effluents from wild-type versus α-gal KO pig lungs (Supplementary Fig. S1).

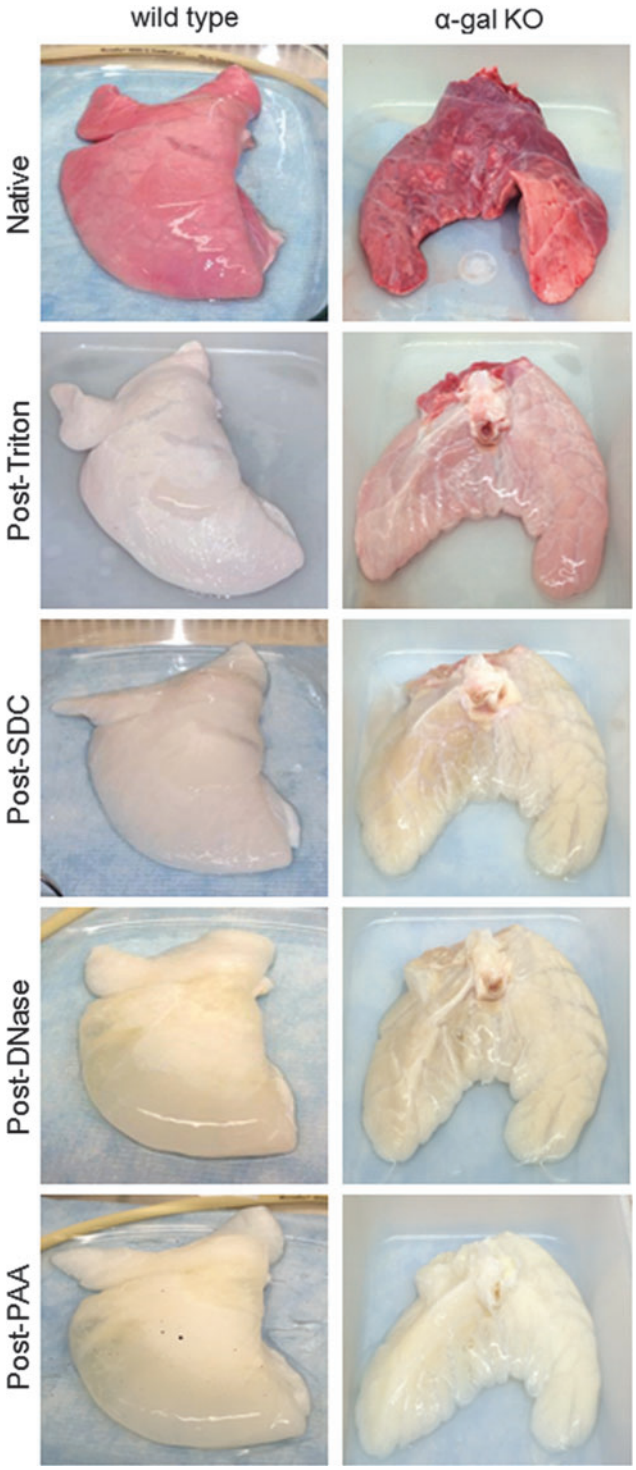

FIG. 1. Wild-type and α-gal KO pig lungs are comparably grossly decellularized. Progressive decellularization results in comparable clearing of blood and pink coloration resulting in final pearly white translucent tissues. Representative images from wild-type ($n=33$) and α-gal KO ($n=17$) pig lungs are shown. α-Gal KO, alpha 1,3 galactosyltransferase knock out; PAA, peracetic acid; SDC, sodium deoxycholate. Color images available online at www.liebertpub.com/tec

IHC staining for major ECM proteins including types 1 and 4 collagen, fibronectin, and laminin, demonstrated general retention with no obvious qualitative differences between decellularized wild-type and α-gal KO pig lungs (Fig. 3A, B). Similar to the EVG stains, immunostaining for elastin was qualitatively decreased and somewhat fragmented appearing in both wild-type and α-gal KO pig lungs. Similar qualitative appearance of residual representative cytoskeletal proteins smooth muscle actin (SMA) and smooth muscle myosin (SMM) was observed in decellularized wild-type and α-gal KO pig lungs (Fig. 3C).

Decellularized wild-type but not α-gal KO pig lungs can display evidence of residual galactosylated proteins or debris

Previously, the α-gal epitope has been detected in both native and decellularized rodent and porcine tissues.[16–20] Histochemical staining for isolectin B4, a standard approach for detecting galactosylated proteins,[28] demonstrates diffuse presence of galactose residues in the native wild-type but not native α-gal KO pig lungs (Fig. 4). As expected, no isolectin B4 staining is observed in decellularized α-gal KO pig lungs. In general, well-decellularized wild-type lungs, as assessed by absence of visible nuclei on H&E stains and by absence of intact DNA on DNA gels, did not have evidence of significant isolectin B4 staining. However, we did observe small sporadic patches of positive isolectin B4 staining, possibly corresponding to residual protein debris or α-galactosylated matrix proteins (Fig. 4). Preadsorbing the lectin with galactose before staining virtually abolished this staining and therefore demonstrates the specificity of this approach.[28] This suggests that residual galactosylated proteins or debris exists in acellular wild-type pig lungs. As expected, there is no isolectin B4 staining observed in decellularized α-gal KO pig lungs. These results suggest that incompletely decellularized or even scattered areas of incomplete decellularization in otherwise well-decellularized lungs could result in retention of potentially immunogenic galactosylated proteins or protein debris (Supplementary Fig. S2).

Mass spectrometric analyses demonstrate minimal differences between protein content of decellularized wild-type versus α-gal KO pig lungs

We have previously demonstrated that semi-quantitative mass spectrometric assessment of trypsin-digested acellular lung scaffolds is a powerful means of assessing many residual proteins, including both ECM and a range of cell-associated proteins, following lung decellularization.[9–12,24–26] While not all proteins can be detected using current techniques, in part due to variability in protein solubility and difficulties in detecting low molecular weight proteins, this is an important technique for reliably assessing comparative differences as well as analyzing trends in residual proteins between different acellular scaffolds obtained from different types of lungs or experimental conditions. We thus compared 6 wild-type and 10 α-gal KO similarly decellularized pig lungs using this approach where proteins were positively identified with two or more unique peptide hits and were subsequently categorized in one of six groups based on cellular or extracellular location: cytosolic, ECM, cytoskeletal, nuclear, membrane-associated, and secreted.[9–12,24–26] Heatmaps were generated

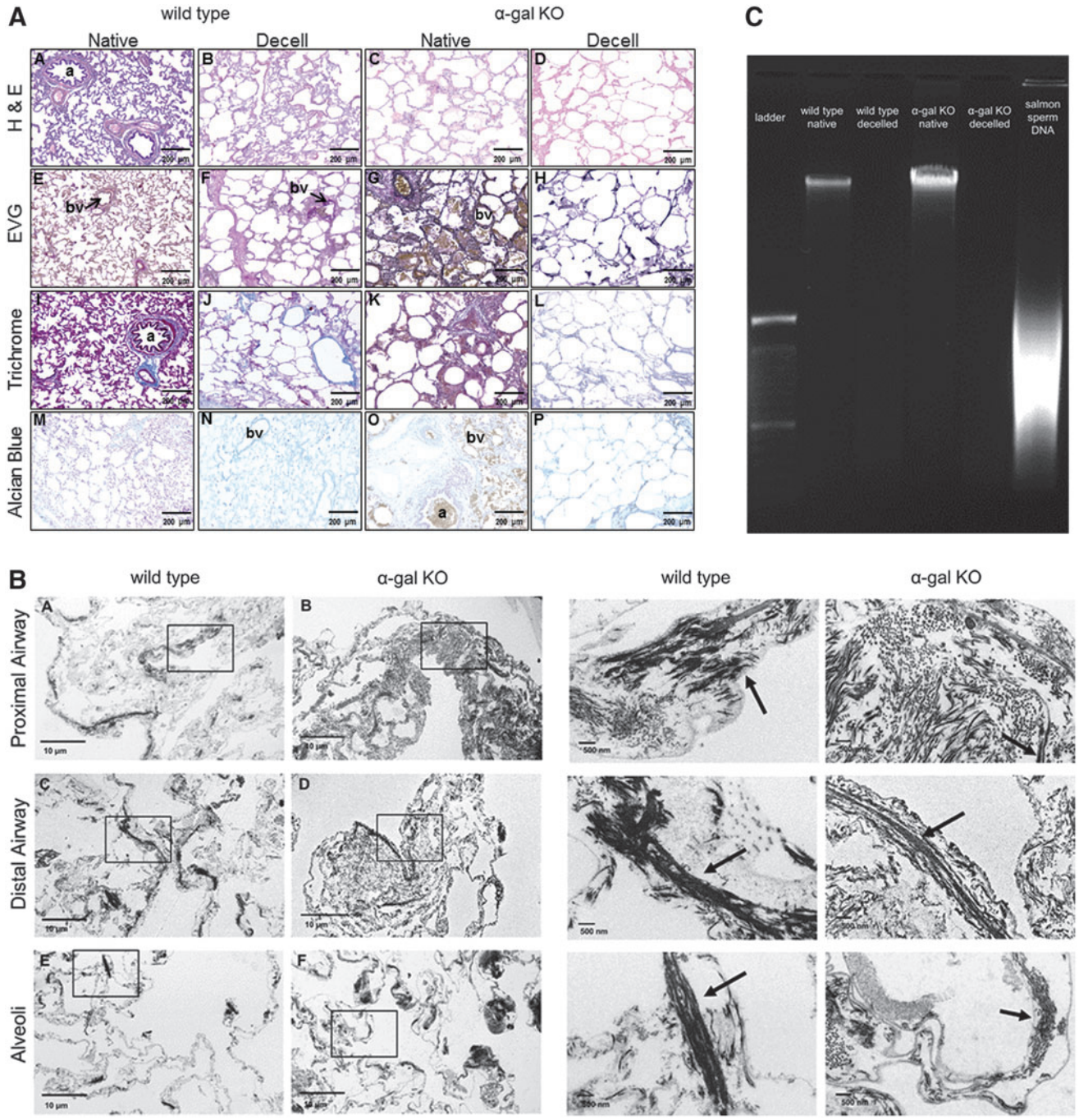

FIG. 2. The decellularization process largely preserves the native structure of porcine lungs. Representative images of native and decellularized wild-type and α-gal KO pig lungs are depicted. **(A)** Photomicrographs demonstrate qualitative preservation of characteristic structure and major ECM proteins (collagen, elastin) by H&E, EVG, and trichrome stains. Glycosaminoglycan content is qualitatively decreased as assessed by Alcian blue staining. Original magnification 100×. Representative images from wild-type ($n=33$) and α-gal KO ($n=17$) pig lungs are shown. **(B)** Transmission electron microscopy demonstrates comparable appearance of proximal airway, distal airway, and alveolar septal regions in decellularized wild-type and α-gal KO pig lungs (scale bar is indicated on each image). Representative images from a single decellularized wild-type and single α-gal KO lung are shown. Enlargements of the *insets* for each image demonstrate more detail in residual collagen and elastin fibers (*arrows*). **(C)** DNA gels demonstrate minimal residual DNA in decellularized wild-type and α-gal KO pig lungs compared to native controls. A DNA ladder and salmon sperm DNA (positive control) are shown for comparison. Representative gels for native and decellularized wild-type and α-gal KO pig lungs are shown. a, airways; bv, blood vessels; ECM, extracellular matrix; EVG, Verhoeff's Van Gieson; H&E, hematoxylin and eosin. Color images available online at www.liebertpub.com/tec

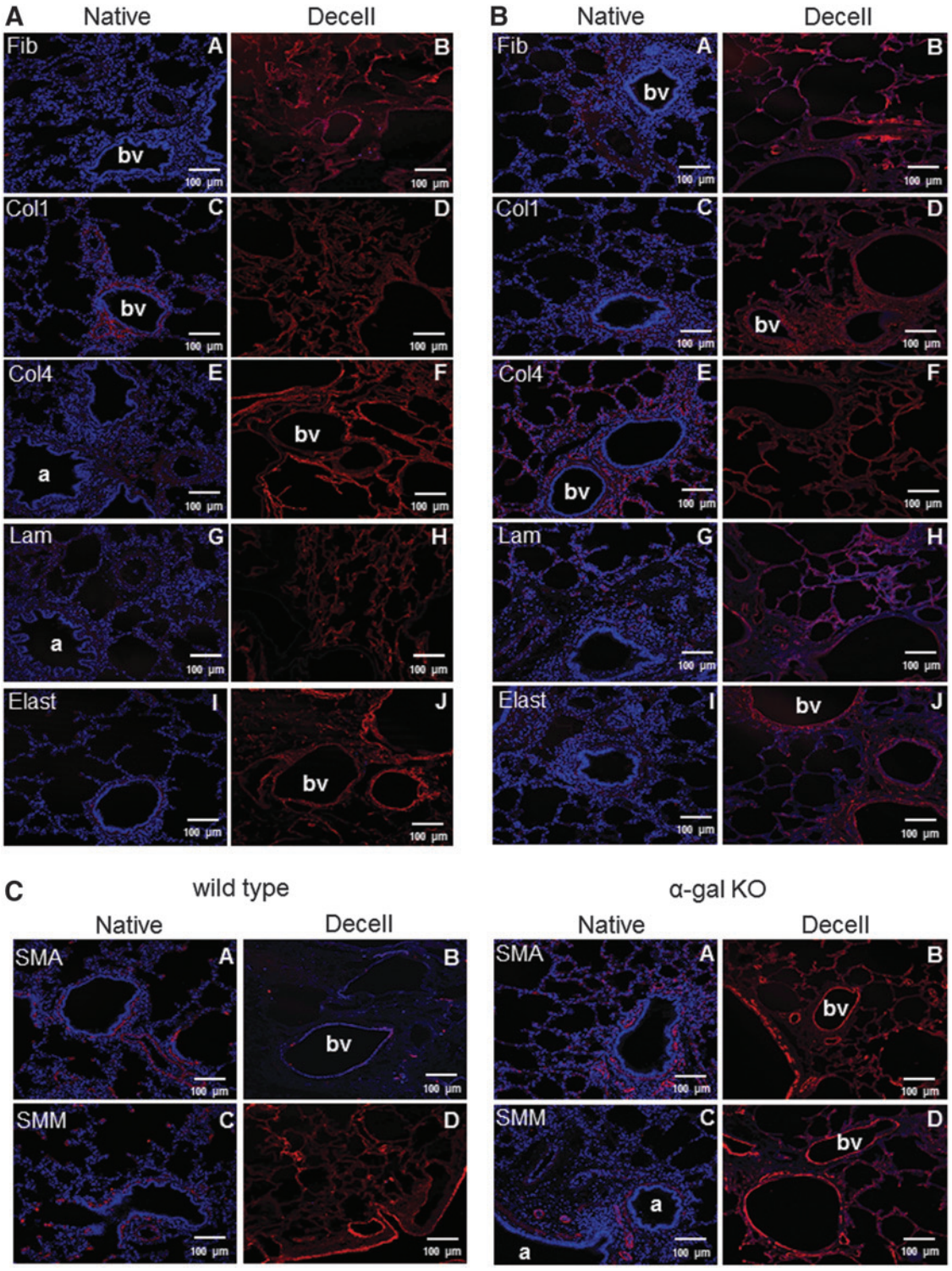

FIG. 3. Decellularization similarly preserves major ECM proteins in wild-type and α-gal KO pig lungs. Representative photomicrographs comparing native and decellularized wild-type and α-gal KO pig lungs are depicted and demonstrate similar qualitative retention of ECM proteins **(A, B)**, SMM, and actin. **(C)** Nuclear DAPI staining is depicted in *blue* and the stain(s) of interest are depicted in *red* or *green*. Original magnifications 100×. Representative images from 2 wild-type and 11 α-gal KO pig lungs are shown. Col1, type I collagen; Col4, type 4 collagen; Elast, elastin; Fib, fibronectin; Lam, laminin; SMA, smooth muscle actin; SMM, smooth muscle myosin. Color images available online at www.liebertpub.com/tec

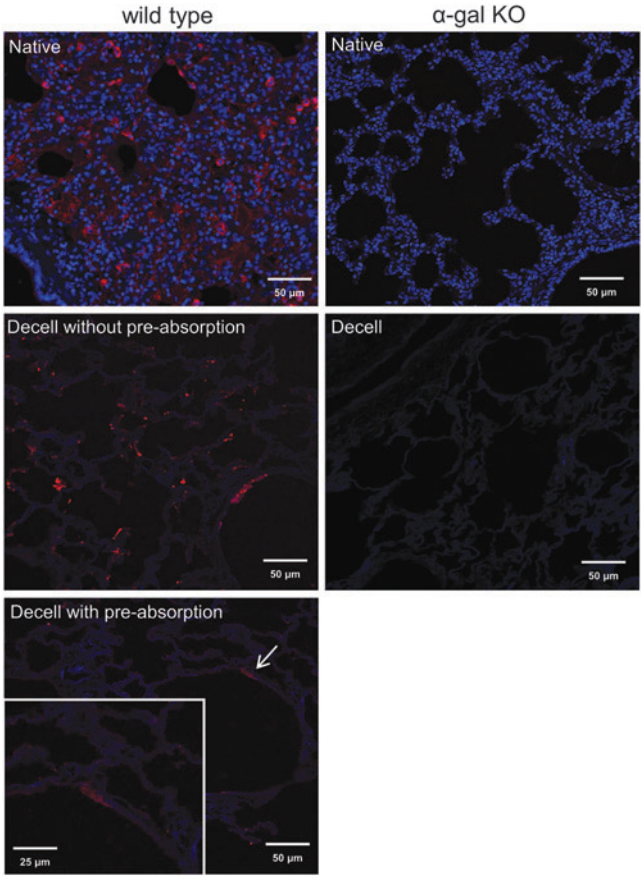

FIG. 4. Isolectin B4 staining demonstrates the potential for residual α-galactosylated proteins or protein debris remaining in decellularized wild-type versus α-gal KO pig lungs. Small areas of positive (*red*) staining (*arrow*, *insert*) can be sporadically observed in what appear to be otherwise well-decellularized wild-type pig lungs as judged by histologic appearance and residual DNA content. In contrast, no lectin staining is observed in either native or decellularized α-gal KO pig lungs. Original magnification 200×. Representative images from 23 wild-type and 18 α-gal KO pig lungs are shown. Color images available online at www.liebertpub.com/tec

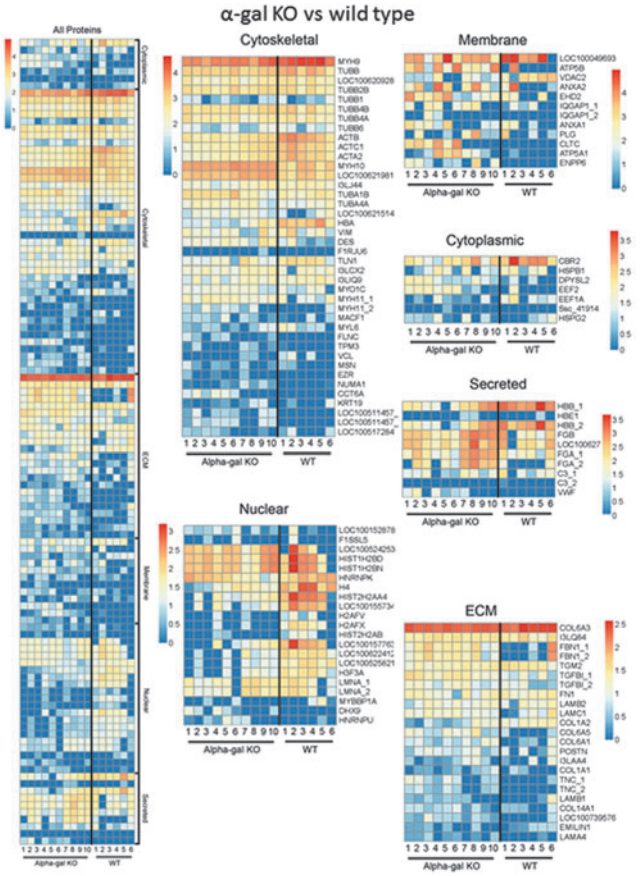

FIG. 5. Mass spectrometric assessment of residual proteins following decellularization of wild-type versus α-gal KO pig lungs demonstrates overall concordance in residual proteins detected. Positively identified proteins in decellularized wild-type versus α-gal KO pig lungs (i.e., those proteins that exceeded the FDR cutoff for identification) from each method of decellularization were assigned to groups according to subcellular location (cytoskeletal, cytosolic, ECM, membrane-associated, nuclear, and secreted). Heatmaps were generated using the log normal transformation of total spectral counts for all positively identified proteins and grouped by category. Representative heatmaps from 6 wild-type and 10 α-gal KO pig lungs are shown. FDR, false discovery rates. Color images available online at www.liebertpub.com/tec

from the log normal transformation of unique peptide hits from each positively identified protein for visual comparison (Fig. 5). Insets for each protein category show more detail than the general patterns depicted in the combined all proteins heatmap. In general, there was good concordance between individual lungs within the wild-type and α-gal KO groups and a similar general detection of important ECM proteins (collagens, laminins) and cytoskeletal proteins (tubulins, myosins) between the groups (Supplementary Tables S2 and S3). However, there were significant differences in ~25% of residual proteins detected in the decellularized wild-type versus α-gal KO lungs. Other statistically significant differences between decellularized wild-type and α-gal KO lungs are summarized in Supplementary Tables S4 and S5. Both decellularized wild-type and α-gal KO lungs variably contained differing amounts of residual cytoskeletal, cytosolic, or nuclear proteins detected by mass spectrometry. This highlights previous observations that even lungs considered well decellularized by criteria such as absence of cells, nuclei, and cell debris on histologic evaluations, and absence of significant amounts of residual DNA may still have a range of retained non-ECM proteins.[29,30]

Human lung epithelial cells, lung fibroblasts, and mesenchymal stromal cells demonstrate comparable seeding patterns, histologic appearance, and viability after inoculation into decellularized wild-type and α-gal KO lungs

Using a high-throughput technique we have previously developed utilizing alginate-coated small segments (~1 cm^3 segments dissected from the decellularized whole pig lungs,[11] we inoculated individual segments with one of four different human cell types including airway epithelial (HBE), vascular endothelial (CBF), lung fibroblasts (HLF), and bone marrow-derived mesenchymal stromal cells (hMSC). Cells were

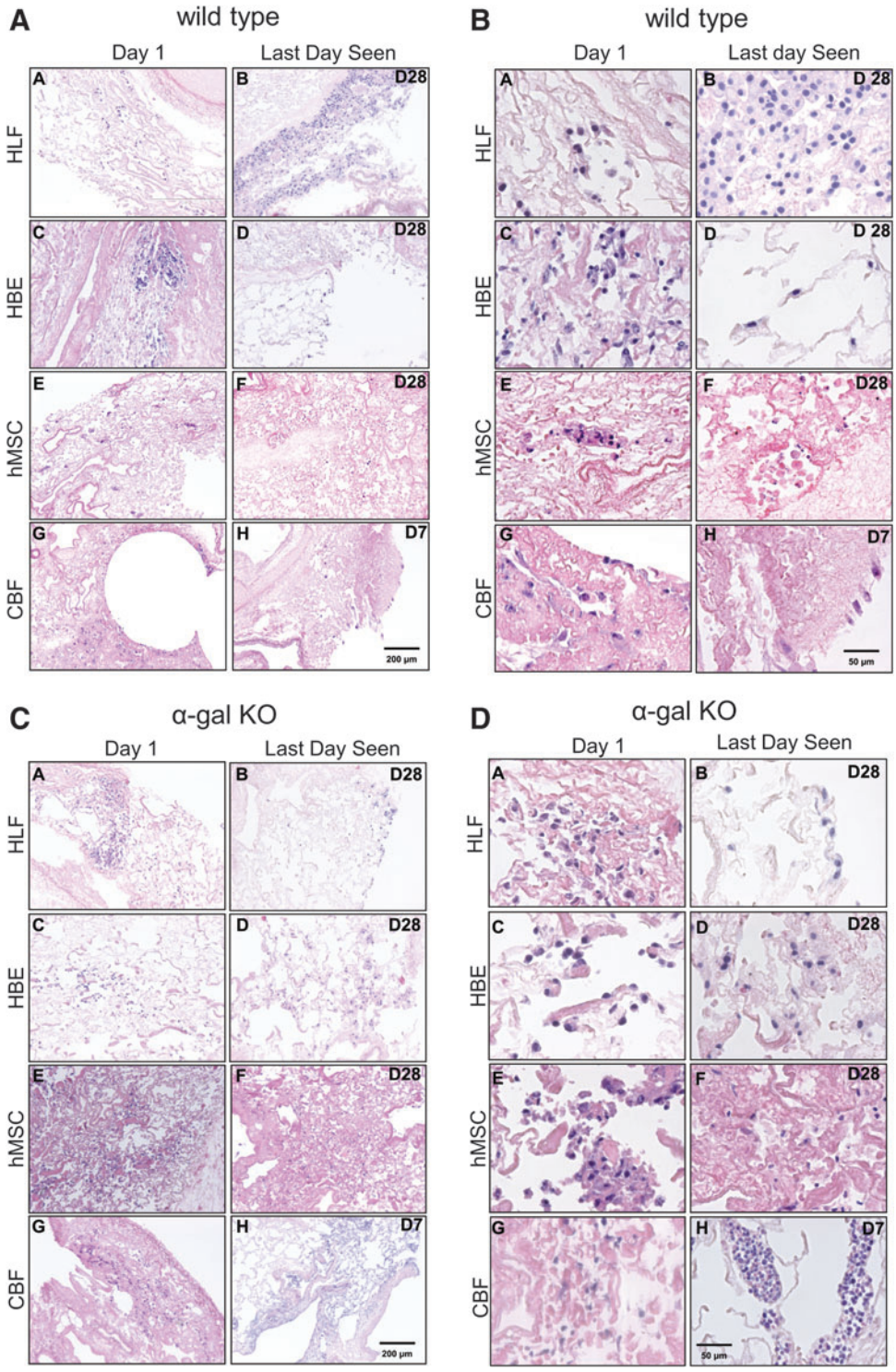

FIG. 6. HBE, hMSC, and HLFs demonstrate comparable seeding patterns and viability for up to 28 days following inoculation into both wild-type and α-gal KO pig lungs, but CBF cells only survive for 7 days. Representative H&E low power (100×) photomicrographs show characteristic recellularization patterns 1 day postinoculation of each cell type (*left column*) and the last day viable cells were observed (*right column*) in acellular wild-type **(A, B)** or α-gal KO **(C, D)** pig lungs. Representative images from 33 wild-type and 17 α-gal KO lungs seeded with each cell type are shown. **(B, D)** High power (400×) images of the respective seedings into either acellular wild-type **(B)** or α-gal KO **(D)** pig lungs. In general, cells that do not interact with the ECM scaffold and remain in the airspaces or vascular spaces unattached to any matrix demonstrated rounding up of cells and nuclear fragmentation, consistent with anoikis or apoptosis. HBE, human bronchial epithelial; HLF, human lung fibroblasts; hMSC, human bone marrow-derived mesenchymal stromal cell. Color images available online at www.liebertpub.com/tec

inoculated into physiologically relevant compartments through either small airways (HBE, HLF, hMSC) or blood vessels (CBF) of the small segments. Following inoculation and overnight incubation of the segments at 37°C, each segment was sliced into approximately 1–2 mm thick sections, each of which was cultured individually, submerged in appropriate cell culture medium for up to 1 month. Initial cell binding and localization as well as growth over the month period were assessed.

One day following airway inoculation of hMSCs, HBEs, or HLFs into either acellular wild-type or α-gal KO scaffolds, HLFs and hMSCs were primarily localized in alveolar spaces and parenchymal regions (Fig. 6A–D, panels A and E). HBEs were also predominantly observed in parenchymal regions (Fig. 6A–D, panel C). Notably, HBEs, as with other cell types that did not engraft to the ECM and remained in the airspaces unattached to any matrix, demonstrated rounding up of cells and nuclear fragmentation,

consistent with anoikis or apoptosis.[24–26] One day after vascular inoculation, the CBFs appeared to be primarily localized in small and medium blood vessels (Fig. 6A–D, panel G).

Viable HBEs, HLFs, and hMSCs were observed through 28 days of culture (Fig. 6A–D, panel B, D, F) without any obvious difference in localization or histologic appearance of cells seeded in wild-type versus α-gal KO scaffolds. In contrast, viable CBFs were only robustly observed through 7 days of culture in both wild-type or α-gal KO scaffolds with only sporadic cells occasionally observed at 28 days (Fig. 6A–D, panel H). At 28 days, HBEs, HLFs, and hMSCs were primarily localized in atelectatic appearing regions of parenchymal lung in both wild-type versus α-gal KO scaffolds although there were scattered areas of cells observed in less atelectatic-appearing areas of alveolar septa. These results are consistent with what we have previously observed following similar cell seedings in decellularized mouse and human lungs.[9–12,24–26] The atelectatic appearance may reflect production of ECM proteins by the cells themselves, contraction of the matrix by the seeded cells, or collapse due to the natural recoil of lung tissue.[26] After 7 days in culture, the CBFs tended to be sparsely localized in blood vessels throughout the lung parenchyma; further, we observed considerably more apoptotic-appearing cells in CBF inoculations than the other three cell types investigated.

Qualitatively assessing proliferation by Ki-67 staining demonstrated scattered positive staining at both day 1 and at day 28 (HBE, HLF, hMSC) or day 7 (CBF) without any obvious difference between cells seeded into wild-type versus α-gal KO scaffolds (Fig. 7A). Qualitatively assessing early apoptosis by caspase-3 staining demonstrated comparable scattered qualitative caspase-3 staining in HBEs and HLFs in both wild-type and α-gal KO lungs at both day 1 and 28 (Fig. 7B). Minimal caspase-3 staining was observed for hMSCs and CBFs seeded into either wild-type or α-gal KO lungs at any time point assessed. Quantitative data analyses of Ki67 and caspase 3 stainings (Fig. 7C) showed no major differences between hMSC seedings into wild-type versus a-gal KO lungs on either day 1 or 28. There was significantly less Ki67 staining and significantly greater caspase-3 staining in CBFs seeded into the α-gal KO scaffolds compared to the wildtype scaffolds on day 1. However, this difference was not apparent on day 28. There was increased Ki67 staining on day 28 in HLFs seeded into the α-gal KO scaffolds. In parallel, there was significantly more caspase-3 staining in day 28 versus day 1 HLF seedings in wild-type scaffolds with a near significant increase in the α-gal KO scaffolds. A similar trend toward increased caspase 3 staining was observed on day 28 seeding of hMSC and CBFs, regardless of scaffold type.

Discussion

To investigate the potential applicability of decellularized pig lungs for xenogeneic lung transplantation approaches, wild-type and α-gal KO pig lungs were decellularized using an optimzied standardized detergent based protocol[9] and compared using qualitative and quantitative histologic, DNA gel and content, IHC, detergent content, and mass spectrometric techniques we have previously utilized to assess decellularized rodent, nonhuman primate, and human lungs.[9–12,24–26] Notably, no consistent significant differences were observed between decellularized wild-type and α-gal KO pig lungs in most endpoints. There were some differences in residual protein content in decellularized wild-type versus α-gal KO pig lungs as assessed by mass spectrometry. Ancillary findings included similar propensity of both wild-type and α-gal KO pig lungs to develop blebs during the decellularization scheme as we have previously noted in pig lungs as compared to rodent or human lungs (data not shown).[9] Whether this resulted from over-pressurization during the constant flow decellularization approach utilized remains unclear as does the implication of bleb formation for potential clinical use of acellular pig lung scaffolds. Ancillary findings also included demonstration of residual cytoskeletal, cytosolic, and nuclear proteins in acellular scaffolds produced from both wild-type and α-gal KO pig lungs. These findings are expected based on our previous, consistent observations of retention of α-SMA and SMM in decellularized rodent, pig, nonhuman primate, and human lungs.[9,10,12,24–26] An important finding of this study is that residual galactosylated proteins and/or debris may be present in wild-type porcine lungs judged to be otherwise well-decellularized by other outcome measures. This suggests that a number of potentially immunogenic cellular proteins can remain in decellularized lungs and promotes consideration of α-gal KO pig lungs for use in xenogeneic lung transplantation approaches. However, as in comparable studies in decellularized rodent and human lungs, this did not appear to affect cell inoculation and behavior in wild-type versus α-gal KO pig lungs. We observed similar initial recellularization and subsequent growth and qualitative appearances over 1 month for two different types of differentiated lung cells and one additional stromal cell population seeded into decellularized wild-type versus α-gal KO pig lungs. In contrast, human pulmonary vascular endothelial cells only survived robustly for a relatively brief period in both wild-type and α-gal KO pig lungs. As further discussed below, there are several potential reasons for the relatively poor survival of the endothelial cells, however, the critical issue for this level of comparison is that they behaved similarly in the α-gal KO as in the wild-type pig lungs. There were some significant differences observed in Ki67 and caspase-3 staining between CBFs seeded into wild-type versus α-gal KO pig lungs at day 1. These might reflect real differences between the lungs or these differences might be attributed to the small sample size and will need to be further explored in a larger study.

Recent progress in approaches for producing and studying decellularized lungs has promoted rapid advances in the field.[2–4] Using an optimized detergent-based approach we have recently developed for large animal and human lungs, and using a combination of histologic, IHC, and mass spectrometric techniques, we and others have found that comparable to decellularization of rodent and human lungs, anatomic structure and the content of major ECM proteins is preserved in decellularized pig lungs.[5,7–9] However, the presence of residual galactosylated proteins and/or debris in lungs judged to be otherwise well-decellularized by other outcome measures suggests that more aggressive decellularization approaches or postdecellularization treatment with α-galactosidases might be necessary to remove the immunogenic α-galactosylated epitopes.[21,22,31,32] Several groups have developed automated decellularization protocols for porcine and human lungs, including large volume rinses between the decellularization

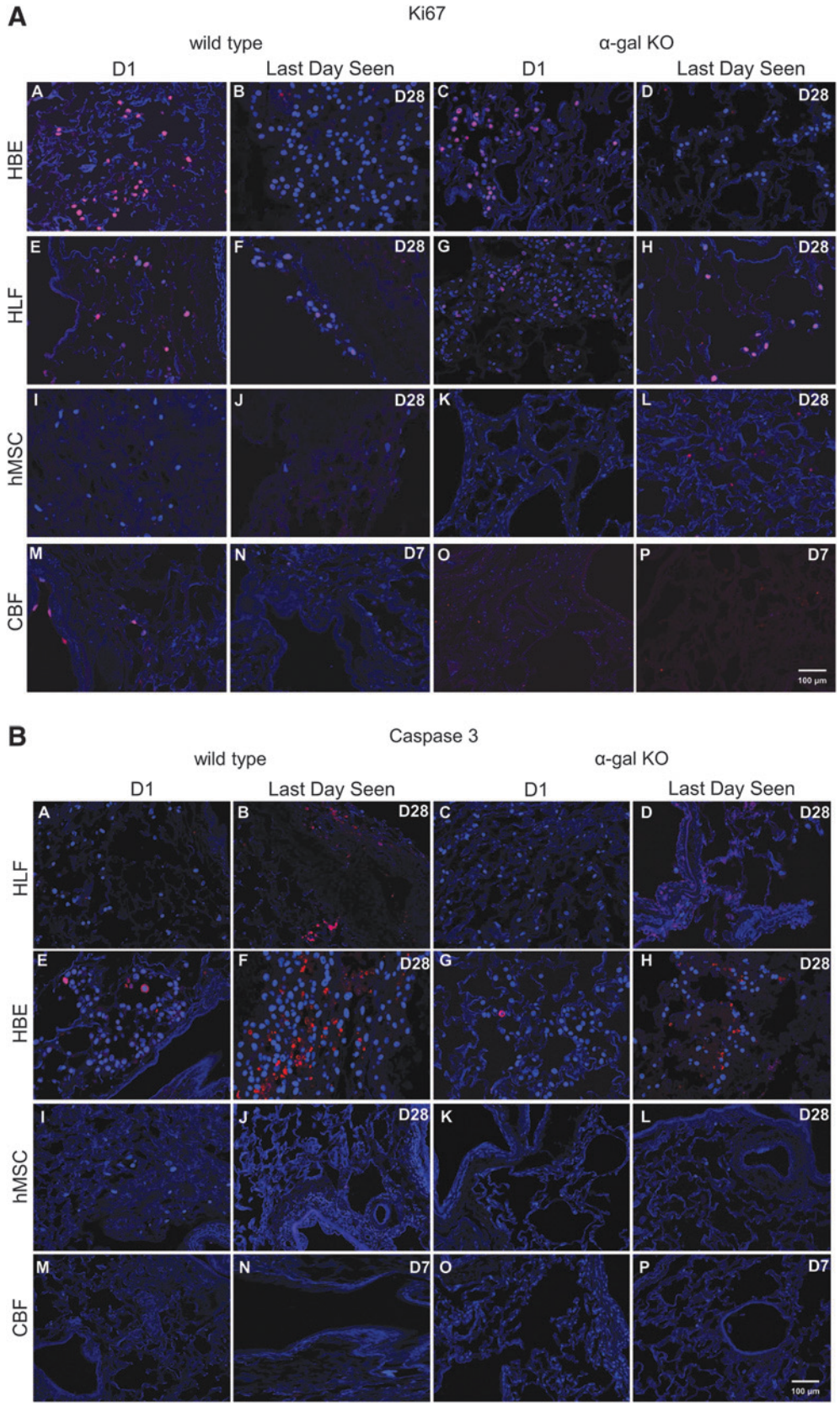

FIG. 7. Cells seeded into wild-type versus α-gal KO pig lungs demonstrate similar patterns of Ki67 and caspase-3 staining. **(A, B)** Representative photomicrographs 1 day postinoculation of each cell type and the last day viable cells were observed are depicted. Original magnification 100×. Ki67 or caspase-3 staining is indicated in *red* and DAPI nuclear staining in *blue*. Representative images from three wild-type and three α-gal KO lungs seeded with each cell type are depicted. **(C)** Quantitative analysis of randomized images from three wild-type and three α-gal KO lungs seeded with each individual cell type. Four regions/slide from each seeding and time point were quantified to determine the percentage of ratio of positive stained Ki67 or caspase-3-expressing cells (*red* staining = Ki67/caspase-3) to total cells (*blue* staining = DAPI). Color images available online at www.liebertpub.com/tec

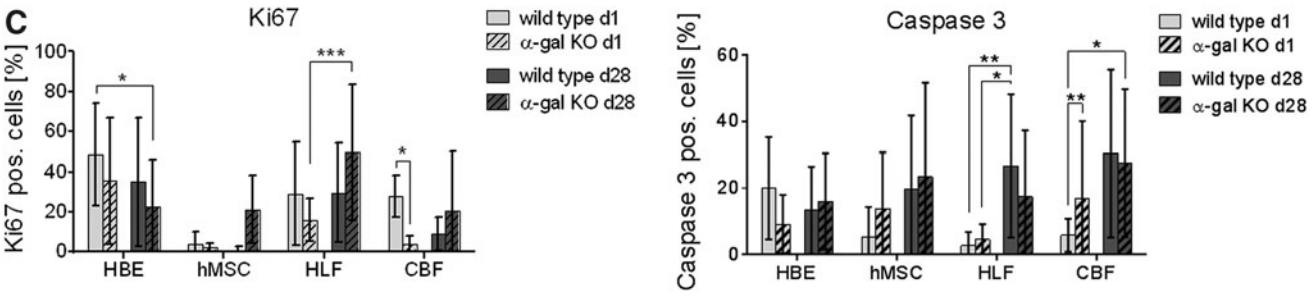

FIG. 7. (Continued).

steps.[5,7,8] These presumably will be more effective at removing residual proteins and debris, but more aggressive decellularization processes might remove components necessary for recellularization, such as growth factors sequestered to the matrix, as well as damaging or degrading the ECM scaffold.[33] Future analyses need to be performed to assess for the immunogenic α-gal epitope and other potentially immunogenic residual proteins in decellularized pig lungs.

Using physiologic inoculation of epithelial, stromal, and endothelial cells into acellular wild-type and α-gal KO pig lungs, we did not observe any differences in initial seeding or in subsequent growth of the inoculated cells over a 1-month period, with the exception of CBF cells, which only lasted in significant numbers until the 7-day time point in both wild-type and α-gal KO acellular pig lungs. Initial proliferation and early apoptosis was different in CBFs seeded into wild-type versus α-gal KO pig lungs although these differences were not apparent at 28 days. This suggests that despite differences in residual proteins detected using the mass spectrometry technique utilized here, an admittedly incomplete assessment of the full range of residual proteins, these proteins do not appear to make a difference in recellularization using the cells and approaches utilized for these studies, by histologic assessment. To fully understand the implications of the range of residual proteins and glycoproteins found in decellularized lungs, further investigation like quantification by western blot and other methods, and functional assessments will help clarify the role of the remaining proteins. This is particularly important given the qualitative information provided by techniques such as IHC assessment of selected residual proteins. In particular, despite a number of recent studies assessing residual proteins in decellularized lungs their functional role, either positively in supporting cell growth and differentiation or negatively in potentially serving as immunogenic foci, remains unclear.

The relatively poor survival of the vascular endothelial cells may reflect several factors including lack of vascular perfusion and also perhaps a nonpermissive environment for the particular cells utilized. Further studies with more primitive endothelial progenitor precursors may provide more robust growth. In parallel, recent advances in perfusion and ventilation approaches for supporting cell growth and function, following seeding of acellular lungs, will allow further support of long-term cell growth.[34,35]

However, there remain many questions for utilizing acellular pig lung scaffolds, particularly those derived from α-gal KO pigs. Our preliminary data investigating seeding with differentiated lung and stromal cells will be followed up with comparable studies using other cell populations, including but not limited to induced pluripotent stem cells and different populations of endogenous lung progenitors. Further study of environmental variables such as mode of perfusion and ventilation is also necessary to optimize recellularization and production of functional lung tissue.

Further, as continued progress is being made in techniques for whole lung de- and recellularization, fundamental questions remain about the potential immunogenicity of the scaffolds, particularly xenogeneic scaffolds. A tenet of the potential use of recellularized lungs is that they will be nonimmunogenic or at least only minimally immunogenic, particularly if recellularized with cells obtained from the eventual transplant recipient. This will reflect both the relative lack of immunogenicity of the decellularized extracellular matrix scaffold and also any potential remodeling by cells seeded into the scaffold that would then mask any potential remaining immunogenic epitopes.[36] As the lung is a more structurally complicated organ than heart valves or skin grafts, it may be more difficult to achieve adequate removal of immunogenic proteins. We are currently assessing potential immunogenicity of both wild-type and α-gal KO pig lung scaffolds in a range of *in vitro* and *in vivo* assays.

Conclusions

Decellularized α-gal KO pig lung scaffolds can be de- and recellularized similar to results observed in wild-type pig lungs. These initial studies provide a firm basis for further investigation into the potential use of α-gal KO pig lung scaffolds for development of xenogeneic transplant approaches.

Methods

Pig lungs

Heart-lung blocs were obtained from euthanized wild-type pigs (14–18 weeks, male *S. scrofa*) through an IACUC-approved organ sharing program at the University of Vermont. Pigs were induced with ketamine and atropine, maintained on isofluorane, and then given an intravenous dose of sodium pentobarbital (Fatal Plus; Vortech Phramaceuticals). Lungs from 15 α-gal KO pigs (6–16 weeks) and 8 older pigs (6 months to 4 years) were obtained from Revivicor, Inc. following euthanasia according to AAALAC approved protocols. Lungs from the younger α-gal KO pig lungs were utilized for decellularization analyses including histologic and mass spectrometric analyses. Five of the α-gal KO pig lungs were incompletely decellularized and thus not utilized for reseeding studies. Well decellularized lungs from both younger and older pigs were utilized for cell

seedings. After euthanasia, the trachea-lung bloc was removed by dissection, the vasculature flushed with sterile saline, packed in ice, and shipped by overnight express. A total of up to 33 wild-type and 23 α-gal KO pig lungs were evaluated for the different components of this study.

Lung decellularization

Pig lungs were decellularized under sterile conditions, using a combined perfusion and physical approach we have recently developed after scaling up and optimizing methods initially developed for rodent and small nonhuman primate models for use in larger pig and human lungs.[9–12,24–26] As previously demonstrated, a constant perfusion rate of 2 L/min yielded optimal results for preserving remaining ECM architecture and protein content while minimizing residual cell debris in decellularized human and porcine lungs content.[9] For each of the below steps, solutions were infused or perfused at a rate of 2 L/min using a roller perfusion pump (Stockert Shiley; SOMA Technologies). On day 1 of the decellularization protocol, the lungs were rinsed six times with 2–3 L for each rinse of deionized (DI) water containing 500 IU/mL penicillin/500 μg/mL streptomycin (5 × pen/strep) (Lonza) through both the trachea and the pulmonary artery. To account for differences in lung or lobe sizes between animals, particularly for larger lungs obtained from older animals, complete filling without overinflating the lungs was used to determine the individual wash volume, resulting in slight variations between lungs. Next, the lungs were rinsed once with Triton solution (4–6 L of 0.1% Triton X-100 [Sigma] and 5 × pen/strep in DI water) infused through both the airways and vasculature. Lungs were filled a second time with Triton solution via both airways and vasculature, submerged in Triton solution, and incubated for 24 h at 4°C on a rocker-shaker (Gene Mate; Bio Express). On day 2, the lungs were removed from the Triton solution and rinsed six times with 2–3 L per rinse of DI water and 5× pen/strep. The lungs were then rinsed once with SDC solution (4–6 L of 2% SDC, [Sigma] in DI water) and SDC solution was then instilled as previously described for day 1. Lungs were incubated in SDC solution for 24 h at 4°C on the rocker-shaker. The next day, lungs were removed from the SDC solution and rinsed six times with 2–3 L per rinse of DI water and 5× pen/strep. The lungs were then rinsed once with sodium chloride (NaCl) solution (4–6 L of 1 M NaCl [USB] and 5× pen/strep in DI water), filled a second time with the NaCl solution, and incubated in the NaCl solution for 1 h at room temperature (25°C) on the rocker-shaker. Lungs were removed from the NaCl solution, rinsed six times with 2–3 L per rinse of DI water and 5× pen/strep as described above. The lungs were then rinsed once with DNAse solution (4–6 L of 30 μg/mL porcine pancreatic DNase [Sigma], 2 mM calcium chloride [$CaCl_2$; Sigma], 1.3 mM magnesium sulfate [$MgSO_4$; Sigma], and 5× pen/strep in DI water), filled a second time with DNAse solution, and incubated for 1 h at room temperature on the rocker-shaker. The lungs were removed from the DNAse solution, rinsed six times with 2–3 L per rinse of DI water and 5× pen/strep as described above, then rinsed once with peracetic acid (PAA) solution (4–6 L of 0.1% [v/v] PAA [Sigma] in 4% [v/v] ethanol solution in DI water), instilled a second time with the PAA solution, and incubated for 1 h at room temperature on the rocker-shaker. Finally, lungs were removed from the PAA solution and rinsed six times with 2–3 L per rinse of DI water and 5× pen/strep as described above. After six washes with 2–3 L of storage solution (in total 12–18 L of a 5× pen/strep, 50 mg/L gentamicin [Cellgro], 2.5 μg/mL amphotericin B [Cellgro] in 1× phosphate-buffered saline [PBS] solution [storage solution] as described for the pen/strep DI water rinses), lungs were stored in storage solution at 4°C until needed, but at maximum for 3 months before use. The protocol steps are summarized in Supplementary Table S1.

Assessment of residual DNA

Native and decellularized lung tissue was dried on tissue paper (Kimwipe, Kimtech; Kimberly-Clark) until no liquid was visibly seen to be released from it, weighed, and DNA was extracted using the DNeasy Blood & Tissue Kit (Qiagen) following the instructions provided by the manufacturer. For qualitative assessment of DNA degradation and size, the same volume of sample per isolated DNA was run on a 0.8% agarose gel and visualized under ultraviolet light with SYBR Safe DNA Gel stain (Invitrogen). A 100 bp ladder and salmon sperm DNA (Invitrogen) was used as DNA size marker and positive control.

Anionic detergent assessment

Concentrations of SDC in wash effluents were determined using our recently published methylene blue (MB) assay.[27] In short, effluent samples were mixed with 0.0125% MB (Sigma-Aldrich) in DI water (w/v) at a ratio of 1:10. After vortexing of the samples with MB, chloroform (Sigma-Aldrich) was added at a ratio of 1:2 (sample:chloroform, v/v). Samples were then vortexed for 1 min. Following a 30 min incubation period at room temperature, 150 μL of the bottom chloroform layer was extracted and the absorbance at 630 nm was measured in a Synergy HT Multi-Detection Microplate Reader (Biotek Instruments) in a polypropylene 96-well plate (Costar). Pure DI-water or PBS (Mediatech, Inc.) containing no detergents served as the blank. SDC concentration was calculated based on SDC standard curves prepared in either DI water (for Triton, SDC, NaCl, and DNAse effluents) or storage solution (for PBS effluents).

Lung histology

Decellularized lungs were fixed with 4% paraformaldehyde for at least 3 h at room temperature, embedded in paraffin, and 5-μm sections mounted on glass slides. Following deparaffinization, sections were stained with H&E, EVG, Masson's Trichrome, or Alcian Blue, and were assessed by standard light microscopy.[9–12,24–26]

Lectin staining

Lung tissue samples were deparaffinized with three 15-min washes in xylene, followed by two 5-min washes in 100% ethanol, two 5-min washes in 95% ethanol, one 5-min wash in 70% ethanol, one 5-min wash in 50% ethanol, one 5-min wash in deionized water, and one 5-min wash in 1% bovine serum albumin (BSA; No. A9647; Sigma) in PBS. Slides were incubated for 60 min with Isolectin GS-IB4 Alexa 568 (No. I21412; Life Technologies) antibody diluted with 1% BSA at a concentration of 20 μg/mL. Some samples

were preabsorbed with galactose during this step, in which case the isolectin antibody preparation was combined with 100 mM galactose (No. S25334; Fisher) before adding to the slides.[28] Following incubation at room temperature, samples were washed five times for 5 min in 1% BSA. The samples were exposed to DAPI (1:500; No. D1306; Invitrogen) in 1% BSA for 15 min. These were washed three times for 5 min in 1% BSA, and a coverslip was applied using Aqua Polymount (No. 18606; Polysciences).[28]

Electron microscopy

For electron microscopic analyses, segments of decellularized porcine lung were fixed overnight at 4°C in Karnovsky's fixative (2.5% glutaraldehyde, 1.0% paraformaldehyde in 0.1 M Cacodylate buffer, pH 7.2). After rinsing in Cacodylate buffer, the tissue was minced into 1 mm^3 pieces and then fixed in 1% osmium tetroxide for 2 h at 4°C. Subsequently, the pieces were rinsed again in Cacodylate buffer, dehydrated through graded ethanols, and then cleared in propylene oxide and embedded in Spurr's epoxy resin (all reagents from Electron Microscopy Sciences). Semithin sections (1 μm) were cut with glass knives on a Reichert ultracut microtome (Reichert-Jung), stained with MB–azure II, and then evaluated for areas of interest (proximal and distal alveolar septae, large/small airways, and blood vessels). Ultrathin sections (60–80 nm) were cut with a diamond knife, retrieved onto 200 mesh thin bar nickel grids, contrasted with uranyl acetate (2% in 50% ethanol) and lead citrate, and examined with a JEOL 1400 TEM (JEOL USA, Inc.) operating at 60 kV.[9]

IHC staining

Standard deparaffinization was performed with three separate 10 min incubations in xylenes, followed by rehydration in a descending series of ethanols, and finally in water. Antigen retrieval was performed by heating tissue in 1× sodium citrate buffer (Dako) at 98°C for 20 min followed by a brief 20 min cool at room temperature. Tissue sections were permeabilized in 0.1% Triton X-100 solution (Sigma-Aldrich) for 15 min. Triton X-100 was removed with two 10 min washes in 1% BSA solution. Blocking was performed with 10% goat serum (Jackson Immuno Research) for 60 min. After blocking, primary antibody was added and tissue sections were incubated overnight at 4°C in a humidified chamber. Tissues were washed three times with 1% BSA (Sigma) solution for 5 min each. Secondary antibody was added and incubated for 60 min at room temperature in a dark humidified chamber. Tissues were again washed three times in 1% BSA solution for 5 min each in the dark. DAPI nuclear stain (Invitrogen/Life Technologies/Thermo Fisher) was added for 5 min at room temperature in the dark followed by two washes in 1% BSA solution for 5 min each. The sections were finally mounted in Aqua Polymount (Lerner Laboratories). Primary antibodies used were as follows: purified mouse anti-fibronectin monoclonal (610077; 1:100; BD Transduction Laboratories), laminin antibody polyclonal (ab11575; 1:100; Abcam), rabbit polyclonal to alpha elastin (ab21607; 1:100; Abcam), SMM heavy chain 2 polyclonal (ab53219; 1:100; Abcam), collagen I polyclonal (ab292; 1:100; Abcam), Ki67 proliferation marker polyclonal (ab16667; 1:50; Abcam), cleaved caspase-3 polyclonal (Asp175; 1:100; Cell Signaling Technology), and mouse clone anti-human actin polyclonal (1A4; 1:10,000; Dako via FAHC). Secondary antibodies used were as follows: Alexa Fluor 568 goat anti-rabbit IgG (H+L) (1:500; Invitrogen), Alexa Fluor 568 $F(ab')_2$ fragment of goat anti-mouse IgG (H+L) (1:500; Invitrogen).[9–11]

For quantitative analyses of KI67 and caspase-3 stainings, slides from three wild-type and three α-gal KO lungs seeded with each individual cell type were analyzed by Image J (http://imagej.nih.gov/ij/index.html). For each seeding and time point, four regions/slide were quantified to determine the percentage of positively stained Ki67 or caspase-3-expressing cells (red staining = Ki67/caspase-3, blue staining = DAPI).

Mass spectrometry

Samples of the same approximate weight and volume, ($\sim$125 mg and 1 cm^3, respectively for each sample), were obtained from similar distal parenchymal regions of lungs. Each sample was dried separately in a SpeedVac and suspended in 40 μL of 100 mM ammonium bicarbonate (NH_4HCO_3) and 50 mM dithiothreitol (DTT) and stored at 56°C for 1 h. After cooling, 5 μL of 500 mM iodoacetamide in 100 mM NH_4HCO_3 was added and the solution was incubated for 30 min at room temperature in the dark, and then dried in a SpeedVac. The dried tissue was suspended in 50 μL of trypsin solution (10 ng/μL) in 50 mM NH_4HCO_3 and incubated overnight at 37°C. Next, 5 μL of 10% formic acid was added to stop the digestion. The sample was centrifuged at 14,000 × *g* for 10 min. Fifteen microliters of supernatant were drawn and desalted using a ZipTip C_{18} (P10; Millipore Corporation) according to the manufacturer's protocol, and then dried in a SpeedVac. The dried peptide samples were dissolved in 20 μL 0.1% formic acid and 2% acetonitrile, and 6 μL was loaded onto a fused silica microcapillary liquid chromatography (LC) column (12 cm 100 μm inner diameter) packed with C18 reversed-phase chromatographic materials (5 μm particle size; 20 nm pore size; Magic C_{18}AQ, Michrom Bioresources, Inc.). Peptides were separated by applying a gradient of 3–60% acetonitrile in 0.1% formic acid for 45 min at a flow rate of 500 nL/min. Nanospray ionization was used to introduce peptides into a linear ion trap (LTQ)-Orbitrap mass spectrometer (Thermo Fisher Scientific) via a nanospray ionization source. Mass spectrometry data were acquired in a data-dependent acquisition mode, in which an Orbitrap survey scan from m/z 400–2000 (resolution: 30,000 full width at half maximum [FWHM] at m/z 400) was paralleled by 10 LTQ tandem mass spectrometry (MS/MS) scans of the most abundant ions.[37] After a liquid chromatography-mass spectrometry (LC-MS) run was completed and spectra were obtained, the spectra were searched against the pig protein sequence database compiled from UniProtKB/Swiss Prot database (www.uniprot.org) in forward and reverse orientations through SEQUEST using Proteome Discoverer software (version 1.4.1.14; Thermo Electron). The search parameters permitted a mass tolerance of 2 and 1 Da for precursor ions (MS1 scans) and fragment ions (MS/MS scans), respectively. Oxidation of methionine (M) and carbamidomethylation of cysteines (C) were allowed as variable modifications. Up to two missed tryptic cleavages of peptides were considered. All search results (msf files) were imported into Scaffold (version Scaffold_4.0.5, Proteome Software, Inc.) for calculations of total spectral counts (Normalized Total Spectral Counts

option was used).[37] Parent mass tolerance of 100 ppm, Protein Threshold of 99%, and Minimum No. of Peptides = 2 were applied to limit the false discovery rates (FDR) to 0% at peptide level in the data set. Proteins that contained identical peptides and could not be differentiated due to the absence of unique peptides were grouped to satisfy the principles of parsimony. Proteins presented are broadly categorized and ranked by the average number of peptides identified from the replicate samples.

Proteins positively identified with two or more unique peptide hits were assigned to one of six groups: ECM, cytosolic, cytoskeletal, nuclear, membrane-associated, and secreted. Heatmaps were generated with the log normal transformation of unique peptide hits from each positively identified protein.[9,10,12] If any of the proteins were matched to more than one category, its predominant subcellular location was chosen for functional grouping. Positive protein identification was assigned based on two or more unique peptide hits within each individual sample, not across all samples.

Preparation and culture of recellularized segments of decellularized lungs

Small, $\sim 2\,cm^3$ pieces of decellularized wild-type and α-gal KO lungs were excised from the larger lobes and blood vessels and/or airways were cannulated with 25 g cannula. After the cannulae were secured with titanium clips (Teleflex Medical) the lung segments were coated in 2.5% sodium alginate (Manugel; FMC Biopolymer) and then immediately cross-linked with a 3% calcium chloride (Sigma) solution, resulting in segments being uniformly coated in a calcium alginate hydrogel.[11] Hydrogel-coated segments were then inoculated with cell suspensions ($1–5 \times 10^6$ cells per segment) and allowed to incubate at 37°C overnight. Segments were then sliced into ~ 1 mm sections with sterile razor blades and each slice placed in a well of a 24-well nontissue culture-treated dish, covered with 2 mL of sterile cell cultivation media, and placed in a standard tissue culture incubator at 37°C with 5% CO_2 as previously described.[11] Slices were harvested at 1, 3, 7, 14, 21, and 28 days postinoculation and fixed for at least 1 h at room temperature in 4% paraformaldehyde. Harvested samples were embedded in paraffin, cut and mounted as 5 μm sections, and then assessed by H&E staining for the presence and distribution of the inoculated cells.

Cells and cell inoculation

HBE cells (courtesy of Albert van der Vliet, University of Vermont, originally from Dr. J. Yankaskas[38]) were cultured on cell culture-treated plastic at 37°C and 5% CO_2 in serum-free culture medium consisting of Dulbecco's modified Eagle medium: nutrient mixture F-12 (DMEM/F-12) 50/50 mix (Corning), 10 ng/mL Cholera toxin (Sigma), 10 ng/mL epidermal growth factor (Sigma), 5 μg/mL insulin (Gemini Bio-Products), 5 μg/mL transferrin (Sigma), 0.1 μM dexamethasone (Sigma), 15 μg/mL bovine pituitary extract (Sigma), 0.5 mg/mL BSA (Life Technologies), and 100 IU/mL penicillin/100 μg/mL streptomycin (Corning). HLF (ATCC, CCL 171) are grown in media consisting of DMEM/F-12 50/50 mix (Corning), 10% fetal bovine serum (Hyclone), 100 IU/mL penicillin/100 μg/mL streptomycin (Corning), and 2 mM L-glutamine (Corning). CBF (pulmonary endothelial colony forming cells) cells were obtained from Mervin Yoder (Indiana University–Purdue University Indianapolis) and grown in cEGM-2 (Lonza) supplemented with 10% fetal bovine serum (Hyclone, Thermo Scientific), and 100 IU/mL penicillin/100 μg/mL streptomycin (Corning). These cells were expanded on collagen type I-coated tissue culture surfaces. hMSCs were obtained from the Texas A&M Stem Cell Core facility. These cells have previously been extensively characterized for cell-surface marker expression and differentiation capacity.[4,39] Cells were expanded in culture using media consisting of Modification of Eagle Medium-Earls Balanced Salt Solution (MEM-EBSS; Hyclone, Thermo Scientific), 20% fetal bovine serum (Hyclone), 100 IU/mL penicillin/100 μg/mL streptomycin (Corning), 2 mM L-glutamine (Corning), and used only until passages 7 or 8.

Statistical analyses

For mass spectrometry assessments, heat maps for the natural log of unique peptide hits for each positively identified protein in the mass spectrometric analyses of lungs decellularized under each experimental condition were generated using the ''pheatmap'' package for ''R'' statistical software version 2.15.1. Comparisons of median unique peptide count between the two groups (alpha-gal vs. wild-type) were done using the nonparametric exact permutation test, with $p < 0.05$ considered statistically significant.[37] This nonparametric equivalent of the *t*-test was used due to the non-normality of the data and the small sample sizes per group. As a measure of agreement/concordance of mass spectrometry proteomic proteins between lungs, nonparametric Spearman correlations were also done, with concordance considered significant at $p < 0.05$.[37] The exact permutation tests and correlations were done using SAS statistical software, version 9.2. Differences between Ki67 or caspase-3 expression were assessed by two-way analysis of variance with Bonferroni post-test.

Acknowledgments

The authors are grateful to Douglas Taatjes, PhD and Nicole Bishop of the UVM Microscopy and Imaging Center for assistance with IHC and lectin staining and interpretations, and to Jason Friedman, Ethan Griswold, Justin Hawk, Robert J. Hommel, Juan Jose Uriarte, and Sean Wrenn for assistance with lung decellularizations. Funding from NIH ARRA RC4HL106625 (D.J.W.), NHLBI R21HL108689 (D.J.W.), the Vermont Lung Center CoBRE grant (P20RR15557), the NIH PACT program (contract HHSN268201000008C), NHBLI Lung Biology Training grant T32 HL076122, NIH Institutional Development Award (IDeA) NIGMS grant P20GM103449, NCRR grant P40RR017447, and United Therapeutics Corporation.

Authors' Contributions

J.P.: Research study design and implementation, data collection and analyses. N.R.B., D.E.W.: Research study design and implementation, data collection and analyses, article writing. F.E.U., A.L.C., T.M., C.P., D.S., Z.D.B., Y.W.L., B.De., J.G.F., R.L.: Data collection and analyses. M.D.: Data analyses (statistical). A.M.H., T.P.: Research study design and implementation. J.B., B.Da.: Provided reagents (transgenic pig lungs). D.J.W.: Project coordinator, research study design and implementation, data collection and analyses, article writing.

Disclosure Statement

T.P. is an employee of United Therapeutics, Inc., sponsor of this study. J.B. is an employee of Revivicor, Inc., a subsidiary of United Therapeutics, Inc. B.Da. is an employee of Exemplar Genetics, a service provider to Revivicor, Inc. D.J.W. has received funding from United Therapeutics to conduct these studies.

References

1. Orens, J.B., and Garrity, E.R. General overview of lung transplantation and review of organ allocation. Proc Am Thorac Soc **6,** 13, 2009.
2. Prakash, Y.S., Tschumperlin, D.J., and Stenmark, K.R. Coming to terms with tissue engineering and regenerative medicine in the lung. Am J Physiol Lung Cell Mol Physiol **309,** L625, 2015.
3. Calle, E.A., Ghaedi, M., Sundaram, S., Sivarapatna, A., Tseng, M.K., and Niklason, L.E. Strategies for whole lung tissue engineering. IEEE Trans Biomed Eng **61,** 1482, 2014.
4. Wagner, D.E., Bonvillain, R.W., Jensen, T., Girard, E.D., Bunnell, B.A., Finck, C.M., Hoffman, A.M., and Weiss, D.J. Can stem cells be used to generate new lungs? Ex vivo lung bioengineering with decellularized whole lung scaffolds. Respirology **18,** 895, 2013.
5. Gilpin, S.E., Guyette, J.P., Gonzalez, G., Ren, X., Asara, J.M., Mathisen, D.J., Vacanti, J.P., and Ott, H.C. Perfusion decellularization of human and porcine lungs: bringing the matrix to clinical scale. J Heart Lung Transplant **33,** 298, 2014.
6. Booth, A.J., Hadley, R., Cornett, A.M., Dreffs, A.A., Matthes, S.A., Tsui, J.L., Weiss, K., Horowitz, J.C., Fiore, V.F., Barker, T.H., Moore, B.B., Martinez, F.J., Niklason, L.E., and White, E.S. Acellular normal and fibrotic human lung matrices as a culture system for in vitro investigation. Am J Respir Crit Care Med **186,** 866, 2012.
7. Nichols, J.E., Niles, J.A., and Cortiella, J. Production and utilization of acellular lung scaffolds in tissue engineering. J Cell Biochem **113,** 2185, 2012.
8. O'Neill, J.D., Anfang, R., Anandappa, A., Costa, J., Javidfar, J., Wobma, H.M., Singh, G., Freytes, D.O., Bacchetta, M.D., Sonett, J.R., and Vunjak-Novakovic, G. Decellularization of human and porcine lung tissues for pulmonary tissue engineering. Ann Thorac Surg **96,** 1046; discussion 1055, 2013.
9. Wagner, D.E., Bonenfant, N.R., Sokocevic, D., DeSarno, M.J., Borg, Z.D., Parsons, C.S., Brooks, E.M., Platz, J.J., Khalpey, Z.I., Hoganson, D.M., Deng, B., Lam, Y.W., Oldinski, R.A., Ashikaga, T., and Weiss, D.J. Three-dimensional scaffolds of acellular human and porcine lungs for high throughput studies of lung disease and regeneration. Biomaterials **35,** 2664, 2014.
10. Wagner, D.E., Bonenfant, N.R., Parsons, C.S., Sokocevic, D., Brooks, E.M., Borg, Z.D., Lathrop, M.J., Wallis, J.D., Daly, A.B., Lam, Y.W., Deng, B., DeSarno, M.J., Ashikaga, T., Loi, R., and Weiss, D.J. Comparative decellularization and recellularization of normal versus emphysematous human lungs. Biomaterials **35,** 3281, 2014.
11. Wagner, D., Fenn, S., Bonenfant, N., Marks, E., Borg, Z., Saunders, P., Oldinski, R., and Weiss, D. Design and synthesis of an artificial pulmonary pleura for high throughput studies in acellular human lungs. Cell Mol Bioeng **7,** 184, 2014.
12. Sokocevic, D., Bonenfant, N.R., Wagner, D.E., Borg, Z.D., Lathrop, M.J., Lam, Y.W., Deng, B., Desarno, M.J., Ashikaga, T., Loi, R., Hoffman, A.M., and Weiss, D.J. The effect of age and emphysematous and fibrotic injury on the re-cellularization of de-cellularized lungs. Biomaterials **34,** 3256, 2013.
13. Parker, M.W., Rossi, D., Peterson, M., Smith, K., Sikstrom, K., White, E.S., Connett, J.E., Henke, C.A., Larsson, O., and Bitterman, P.B. Fibrotic extracellular matrix activates a profibrotic positive feedback loop. J Clin Invest **124,** 1622, 2014.
14. Galili, U. Discovery of the natural anti-Gal antibody and its past and future relevance to medicine. Xenotransplantation **20,** 138, 2013.
15. Galili, U. Avoiding detrimental human immune response against Mammalian extracellular matrix implants. Tissue Eng Part B Rev **21,** 231, 2015.
16. Chiang, T.R., Fanget, L., Gregory, R., Tang, Y., Ardiet, D.L., Gao, L., Meschter, C., Kozikowski, A.P., Buelow, R., and Vuist, W.M. Anti-Gal antibodies in humans and 1,3alpha-galactosyltransferase knock-out mice. Transplantation **69,** 2593, 2000.
17. Lee, C., Ahn, H., Kim, S.H., Choi, S.Y., and Kim, Y.J. Immune response to bovine pericardium implanted into alpha1,3-galactosyltransferase knockout mice: feasibility as an animal model for testing efficacy of anticalcification treatments of xenografts. Eur J Cardiothorac Surg **42,** 164, 2012.
18. Park, C.S., Oh, S.S., Kim, Y.E., Choi, S.Y., Lim, H.G., Ahn, H., and Kim, Y.J. Anti-alpha-Gal antibody response following xenogeneic heart valve implantation in adults. J Heart Valve Dis **22,** 222, 2013.
19. Dalmasso, A.P., Vercellotti, G.M., Fischel, R.J., Bolman, R.M., Bach, F.H., and Platt, J.L. Mechanism of complement activation in the hyperacute rejection of porcine organs transplanted into primate recipients. Am J Pathol **140,** 1157, 1992.
20. Kasimir, M.T., Rieder, E., Seebacher, G., Wolner, E., Weigel, G., and Simon, P. Presence and elimination of the xenoantigen gal (alpha1,3) gal in tissue-engineered heart valves. Tissue Eng **11,** 1274, 2005.
21. Choi, S.Y., Jeong, H.J., Lim, H.G., Park, S.S., Kim, S.H., and Kim, Y.J. Elimination of alpha-gal xenoreactive epitope: alpha-galactosidase treatment of porcine heart valves. J Heart Valve Dis **21,** 387, 2012.
22. Xu, H., Wan, H., Zuo, W., Sun, W., Owens, R.T., Harper, J.R., Ayares, D.L., and McQuillan, D.J. A porcine-derived acellular dermal scaffold that supports soft tissue regeneration: removal of terminal galactose-alpha-(1,3)-galactose and retention of matrix structure. Tissue Eng Part A **15,** 1807, 2009.
23. Mohiuddin, M.M., Singh, A.K., Corcoran, P.C., Hoyt, R.F., Thomas, M.L., 3rd, Ayares, D., and Horvath, K.A. Genetically engineered pigs and target-specific immunomodulation provide significant graft survival and hope for clinical cardiac xenotransplantation. J Thorac Cardiovasc Surg **148,** 1106; discussion 1113, 2014.
24. Wallis, J.M., Borg, Z.D., Daly, A.B., Deng, B., Ballif, B.A., Allen, G.B., Jaworski, D.M., and Weiss, D.J. Comparative assessment of detergent-based protocols for mouse lung decellularization and re-cellularization. Tissue Eng Part C Methods **18,** 420, 2012.
25. Bonvillain, R.W., Danchuk, S., Sullivan, D.E., Betancourt, A.M., Semon, J.A., Eagle, M.E., Mayeux, J.P., Gregory, A.N., Wang, G., Townley, I.K., Borg, Z.D., Weiss, D.J., and Bunnell, B.A. A nonhuman primate model of lung regeneration: detergent-mediated decellularization and initial in vitro recellularization with mesenchymal stem cells. Tissue Eng Part A **18,** 2437, 2012.
26. Daly, A.B., Wallis, J.M., Borg, Z.D., Bonvillain, R.W., Deng, B., Ballif, B.A., Jaworski, D.M., Allen, G.B., and

Weiss, D.J. Initial binding and recellularization of decellularized mouse lung scaffolds with bone marrow-derived mesenchymal stromal cells. Tissue Eng Part A **18,** 1, 2012.
27. Zvarova, B., Uhl, F.E., Uriarte, J.J., Borg, Z.D., Coffey, A.L., Bonenfant, N.R., Weiss, D.J., and Wagner, D.E. Residual detergent detection method for nondestructive cytocompatibility evaluation of decellularized whole lung scaffolds. Tissue Eng Part C Methods **22,** 418, 2016.
28. Taatjes, D.J., Barcomb, L.A., Leslie, K.O., and Low, R.B. Lectin binding patterns to terminal sugars of rat lung alveolar epithelial cells. J Histochem Cytochem **38,** 233, 1990.
29. Crapo, P.M., Gilbert, T.W., and Badylak, S.F. An overview of tissue and whole organ decellularization processes. Biomaterials **32,** 3233, 2011.
30. Li, Q., Uygun, B.E., Geerts, S., Ozer, S., Scalf, M., Gilpin, S.E., Ott, H.C., Yarmush, M.L., Smith, L.M., Welham, N.V., and Frey, B.L. Proteomic analysis of naturally-sourced biological scaffolds. Biomaterials **75,** 37, 2016.
31. Lim, H.G., Choi, S.Y., Yoon, E.J., Kim, S.H., and Kim, Y.J. In vivo efficacy of alpha-galactosidase as possible promise for prolonged durability of bioprosthetic heart valve using alpha1,3-galactosyltransferase knockout mouse. Tissue Eng Part A **19,** 2339, 2013.
32. Kim, M.S., Jeong, S., Lim, H.G., and Kim, Y.J. Differences in xenoreactive immune response and patterns of calcification of porcine and bovine tissues in alpha-Gal knock-out and wild-type mouse implantation models. Eur J Cardiothorac Surg **48,** 392, 2015.
33. Shojaie, S., Ermini, L., Ackerley, C., Wang, J., Chin, S., Yeganeh, B., Bilodeau, M., Sambi, M., Rogers, I., Rossant, J., Bear, Christine E., and Post, M. Acellular lung scaffolds direct differentiation of endoderm to functional airway epithelial cells: requirement of matrix-bound HS proteoglycans. Stem Cell Reports **4,** 419, 2015.
34. Ren, X., Moser, P.T., Gilpin, S.E., Okamoto, T., Wu, T., Tapias, L.F., Mercier, F.E., Xiong, L., Ghawi, R., Scadden, D.T., Mathisen, D.J., and Ott, H.C. Engineering pulmonary vasculature in decellularized rat and human lungs. Nat Biotechnol **33,** 1097, 2015.
35. Charest, J.M., Okamoto, T., Kitano, K., Yasuda, A., Gilpin, S.E., Mathisen, D.J., and Ott, H.C. Design and validation of a clinical-scale bioreactor for long-term isolated lung culture. Biomaterials **52,** 79, 2015.
36. Keane, T.J. and Badylak, S.F. The host response to allogeneic and xenogeneic biological scaffold materials. J Tissue Eng Regen Med **9,** 504, 2015.
37. Nesvizhskii, A.I., Keller, A., Kolker, E., and Aebersold, R. A statistical model for identifying proteins by tandem mass spectrometry. Anal Chem **75,** 4646, 2003.
38. Yankaskas, J.R., Haizlip, J.E., Conrad, M., Koval, D., Lazarowski, E., Paradiso, A.M., Rinehart, C.A., Jr., Sarkadi, B., Schlegel, R., and Boucher, R.C. Papilloma virus immortalized tracheal epithelial cells retain a well-differentiated phenotype. Am J Physiol **264,** C1219, 1993.
39. Sekiya, I., Larson, B.L., Smith, J.R., Pochampally, R., Cui, J.G., and Prockop, D.J. Expansion of human adult stem cells from bone marrow stroma: conditions that maximize the yields of early progenitors and evaluate their quality. Stem Cells **20,** 530, 2002.

Address correspondence to:
Daniel J. Weiss, MD, PhD
Department of Medicine
University of Vermont College of Medicine
149 Beaumont Avenue, HSRF 226
Burlington, VT 05405

E-mail: dweiss@uvm.edu

Received: March 21, 2016
Accepted: June 2, 2016
Online Publication Date: July 11, 2016